Current Biology 20, 1945–1952, November 9, 2010 ©2010 Elsevier Ltd All rights reserved DOI 10.1016/j.cub.2010.09.065

Report

Nucleoredoxin Sustains Wnt/β-Catenin Signaling by Retaining a Pool of Inactive Dishevelled Protein

Yosuke Funato,[1] Takeshi Terabayashi,[1,4] Reiko Sakamoto,[3] Daisuke Okuzaki,[2] Hirotake Ichise,[3] Hiroshi Nojima,[2] Nobuaki Yoshida,[3] and Hiroaki Miki[1,*]

[1]Laboratory of Intracellular Signaling, Institute for Protein Research

[2]Department of Molecular Genetics, Research Institute for Microbial Diseases

Osaka University, Suita, Osaka 565-0871, Japan

[3]Laboratory of Developmental Genetics, Center for Experimental Medicine and Systems Biology, Institute of Medical Science, University of Tokyo, Minato-ku, Tokyo 108-8639, Japan

Summary

Overexpression of Dishevelled (Dvl), an essential component of the Wnt signaling pathway, is frequently associated with tumors [1, 2], and thus the Dvl protein level must be tightly controlled to sustain Wnt signaling without causing tumors. Kelch-like 12 (KLHL12) targets Dvl for ubiquitination and degradation [3], suggesting its potential importance in avoiding aberrant Dvl overexpression. However, the regulatory mechanism of the KLHL12 activity remained elusive. We show here that nucleoredoxin (NRX) determines the Dvl protein level, which is revealed by analyses on *NRX*$^{-/-}$ mice showing skeletal and cardiovascular defects. Consistent with the previously reported Dvl-inhibiting function of NRX [4], Wnt/β-catenin signaling is hyperactivated in *NRX*$^{-/-}$ osteoblasts. However, the signal activity is suppressed in cardiac cells, where KLHL12 is highly expressed. Biochemical analyses reveal that Dvl is rapidly degraded by accelerated ubiquitination in *NRX*$^{-/-}$ mouse embryonic fibroblasts, and they fail to activate Wnt/β-catenin signaling in response to Wnt ligands. Moreover, experiments utilizing purified proteins show that NRX expels KLHL12 from Dvl and inhibits ubiquitination. These findings reveal an unexpected function of NRX, retaining a pool of inactive Dvl for robust activation of Wnt/β-catenin signaling upon Wnt stimulation.

Results and Discussion

NRX Knockout Is Perinatally Lethal

We previously reported that nucleoredoxin (NRX) directly binds to Dishevelled (Dvl) and inhibits its signaling function in culture cells [4]. To further elucidate the function of NRX in vivo, we generated *NRX* knockout mice. A redox-catalytic motif (WCPPC) in NRX is essential for NRX-Dvl interaction and Wnt/β-catenin signaling suppression [4]. Therefore, we targeted exons 3 and 4, which include the coding region of this catalytic motif, by homologous recombination using a gene cassette containing *LacZ* and neomycin-resistance genes (see Figure S1A available online). Successful recombination was confirmed by Southern blotting (Figure S1B). We found that *NRX* knockout is perinatally lethal (Figure S1C)—a result consistent with a previously reported finding about mice carrying hypomorphic *NRX* alleles with a splice-site mutation [5].

Aberrant Activation of Wnt/β-Catenin Signaling in Osteoblasts from *NRX*$^{-/-}$ Mice

On embryonic day (E) 18.5, *NRX*$^{-/-}$ embryos were smaller than their *NRX*$^{+/+}$ littermates (Figure S1D). Further, many of them exhibited craniofacial defects with short frontal regions. By staining the bones and cartilages of the embryos, we confirmed that their frontal bones were significantly shorter than those of their *NRX*$^{+/+}$ littermates (Figure 1A). Further analyses of the bone preparations revealed sternal defects (Figure S1E). Similar defects in the frontal bones and the sternum have been reported to occur in mouse knockouts of *Axin2* [6] and *GSK3β* [7], which are also suppressors of Wnt/β-catenin signaling. These phenotypic abnormalities appear to be consistent with the inhibitory role of NRX in Wnt/β-catenin signaling.

Yu et al. reported that the craniofacial defects in *Axin2*$^{-/-}$ mice are due to the aberrant activation of Wnt/β-catenin signaling and the resultant excessive osteoblast differentiation and premature ossification and suture closure [6]. Therefore, we assessed differentiation of cells isolated from calvaria of E18.5 embryos. As expected, differentiated osteoblasts were more numerous in the cells from *NRX*$^{-/-}$ embryos than in the cells from *NRX*$^{+/+}$ littermates (Figure 1B). Immunoblotting with an antibody that recognizes the activated β-catenin (ABC) showed that the Wnt/β-catenin pathway was more strongly activated in the cells from the *NRX*$^{-/-}$ embryos (Figure 1C). We then determined whether NRX is expressed in the frontal bone region in vivo. Because the targeted allele includes *LacZ*, whose expression is controlled by the *NRX* gene promoter, we performed LacZ staining of E18.5 embryos and detected positive signals in the frontal bone region (Figure 1D). Immunostaining with the anti-ABC antibody yielded stronger signals for cells in this region. These cells were confirmed as osteoblasts by immunostaining for Runx2, an osteoblast marker (Figure 1E). To further validate the activation of Wnt/β-catenin signaling, we also performed immunostaining for collagen I, a direct transcriptional target for β-catenin [8]. As shown in Figure 1F, we observed a clear augmentation of collagen I signals in the bone region. Collectively, these results suggest that the abnormal bone morphology in *NRX*$^{-/-}$ mice may be caused by aberrant activation of Wnt/β-catenin signaling.

Microarray Transcriptome Analyses

To further explore the defects of *NRX*$^{-/-}$ mice, we performed microarray analyses of E9.5 and E11.5 embryos. No known target genes of Wnt/β-catenin signaling were commonly upregulated in *NRX*$^{-/-}$ mice, but several target genes, such as *Fzd2* and *Occludin* [9], were rather commonly downregulated (Figure S2A). Furthermore, several other target genes, such as *TCF1* and *Brachury(T)* [9, 10], were also downregulated in

*Correspondence: hmiki@protein.osaka-u.ac.jp

[4]Present address: Department of Kidney Development, Institute of Molecular Embryology and Genetics, Kumamoto University, Honjo, Kumamoto 860-0811, Japan

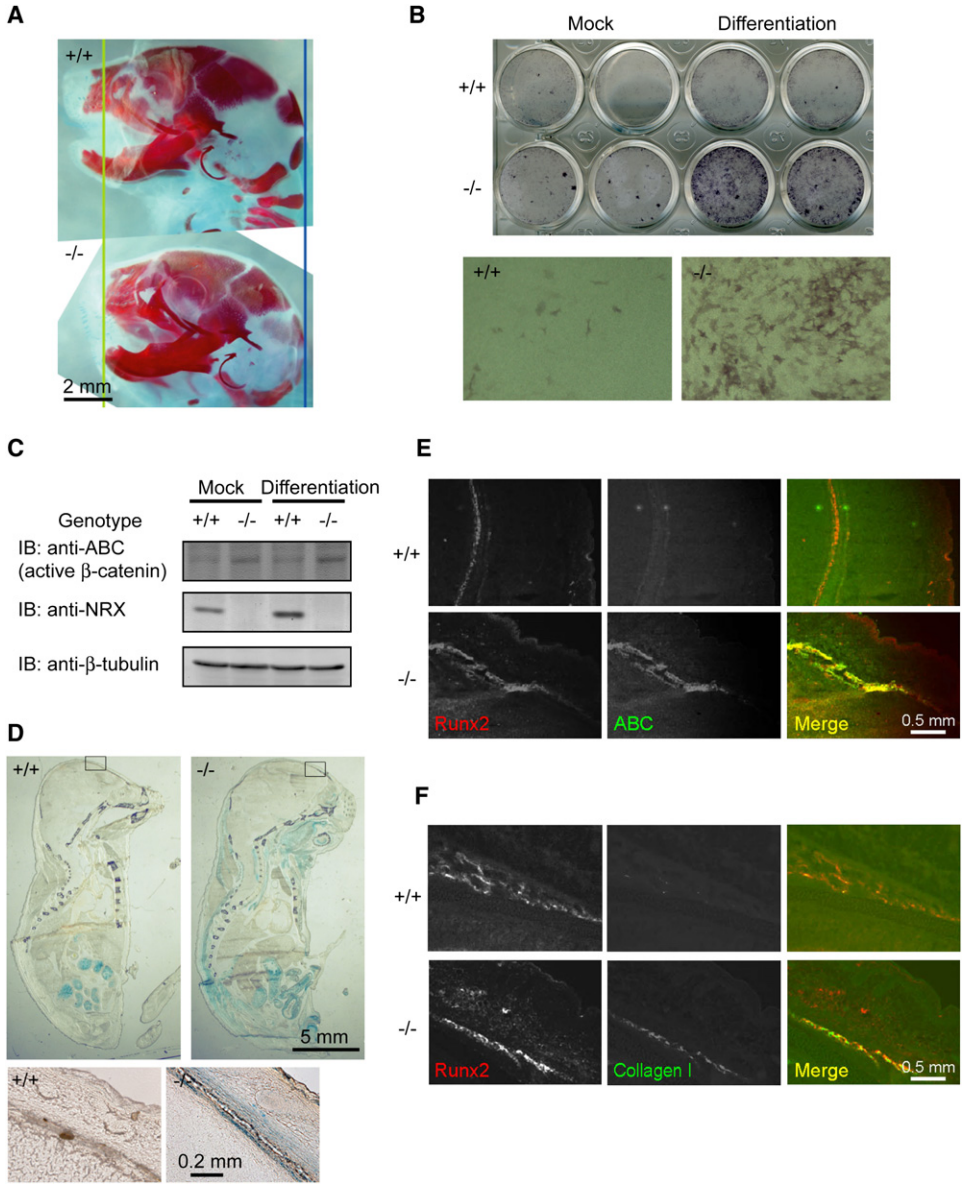

Figure 1. Aberrant Differentiation of Osteoblasts in *NRX*$^{-/-}$ Mice

(A) The cranial region of the skeletal preparations of E18.5 embryos stained by Alizarin red and Alcian blue. The green line is set at the anterior end of the *NRX*$^{-/-}$ skull.

(B) Cells isolated from calvaria of E18.5 embryos were cultured for 5 days in mock media or differentiation media, and differentiated osteoblasts were visualized by alkaline phosphatase staining. Magnified images are also indicated below.

(C) Cells isolated and treated as described in (B) were harvested, and the lysates were subjected to immunoblotting with the indicated antibodies.

(D) Sections of E18.5 embryos were subjected to LacZ staining. The boxed areas are magnified and indicated at the bottom.

(E) Sections were immunostained with anti-Runx2 and anti-ABC antibodies. A merged image (Runx2: red, ABC: green) is also indicated.

(F) Sections were immunostained with anti-Runx2 and anti-collagen I antibodies. A merged image (Runx2: red, collagen I: green) is also indicated.

See also Figure S1.

either E9.5 or E11.5 *NRX*$^{-/-}$ embryos (data not shown). These results suggest that some steps of the Wnt/β-catenin pathway may be inhibited in *NRX*$^{-/-}$ embryos.

Abnormal Cardiovascular Development in *NRX*$^{-/-}$ Mice

Fzd2 is dramatically upregulated during cardiogenesis [11]. Therefore, we examined cardiac morphology in the E18.5 embryos. As shown in Figure 2A, all *NRX*$^{-/-}$ embryos (11 of 11 analyzed) showed a ventricular septal defect (VSD), a hole between the right and left ventricles. More severe defects, e.g., persistent truncus arteriosus (PTA, a defect in the division of the aorta and pulmonary arteries), were also observed in 3 of 11 embryos. Cardiac defects were not observed in the *NRX*$^{+/+}$ and *NRX*$^{+/-}$ embryos. The ventricular septum of the murine heart divides two ventricles at about E14.5. In our study, on E14.5, the *NRX*$^{-/-}$embryos showed septal defects, whereas their *NRX*$^{+/+}$ littermates showed fully formed septa (Figure 2B). Similar defects during cardiovasculogenesis occurred in the *Dvl2*$^{-/-}$ and *Dvl3*$^{-/-}$ mice [12, 13], suggesting that these defects were due to reduction in Wnt/β-catenin signaling

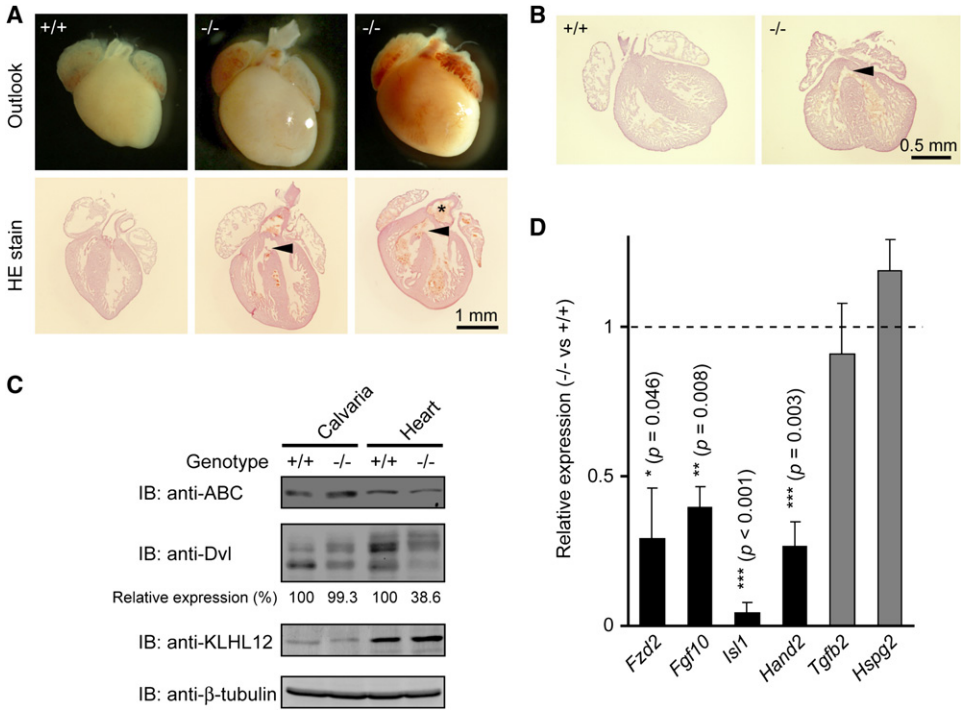

Figure 2. Cardiovascular Defects in *NRX*$^{-/-}$ Embryos

(A) Outlook and Hematoxylin and Eosin (HE)-stained sections of heart from E18.5 embryos. The arrowheads and an asterisk indicate ventricular septal defect (VSD) and persistent truncus arteriosus (PTA), respectively.

(B) HE-stained sections of heart from E14.5 embryos. The arrowhead indicates VSD.

(C) Lysates of cells obtained from calvaria (E18.5) and heart (E10.5) were subjected to immunoblotting with the indicated antibodies. Relative expression levels of the Dishevelled (Dvl) proteins are also indicated by normalizing the levels in *NRX*$^{+/+}$ samples to 100.

(D) The expression levels of various known target genes of the Wnt/β-catenin pathway (black bars) and the Wnt/PCP pathway (gray bars) in embryonic heart (E10.5) were determined by real-time polymerase chain reaction (PCR) experiments. The relative expression levels of *NRX*$^{-/-}$ versus *NRX*$^{+/+}$ are shown as mean ± standard error (SE; n = 3). p values were determined by the two-tailed Student's t test (paired). *p < 0.05, **p < 0.01, ***p < 0.001.

See also Figure S2.

activity. Therefore, we examined β-catenin activation in the embryonic heart by immunoblotting with the anti-ABC antibody; this activation was slightly but significantly reduced in the *NRX*$^{-/-}$ embryos (Figure 2C). Immunoblotting with an anti-Dvl antibody, which recognizes all three mammalian Dvl isoforms (Dvl1, Dvl2, and Dvl3) equally [4], revealed that the cardiac Dvl protein levels were also dramatically reduced in the heart of *NRX*$^{-/-}$ embryos.

Neural crest cells contribute to cardiovascular development, and Wnt/β-catenin signaling is important for their development and migration [14, 15]. We examined whether the distribution of neural crest cells is perturbed in *NRX*$^{-/-}$ embryos, but we failed to detect any significant differences (Figures S2B–S2D).

Cardiovascular development is a complex process, and the importance of the Wnt/β-catenin and Wnt/PCP pathways for this process is well accepted [16]. To identify which pathway was affected in *NRX*$^{-/-}$ embryos, we performed quantitative PCR analyses targeting various genes essential for cardiovascular development. Among these genes, the expression of *Fzd2*, *Fgf10, Isl1*, and *Hand2*, targeted by the Wnt/β-catenin pathway [11, 17], was markedly reduced in the *NRX*$^{-/-}$ embryonic heart, but no significant differences were found in the expression of *Tgfb2* and *Hspg2*, target genes of the Wnt/PCP pathway [18] (Figure 2D). Furthermore, no differences were found in the activation status of Rac and Rho, important mediators of the Wnt/PCP pathway [19] (data not shown).

Wnt-Stimulated Signaling Activity Is Impaired in *NRX*$^{-/-}$ Mouse Embryonic Fibroblasts

The results shown in Figure 2 suggest that the Wnt/β-catenin pathway is impaired in several types of cells or tissues in *NRX*$^{-/-}$ mice. Thus, we isolated mouse embryonic fibroblasts (MEFs) and subjected them to more-detailed analyses at the molecular level. We examined the expression levels of Dvl and found their significant reduction in *NRX*$^{-/-}$ MEFs relative to *NRX*$^{+/+}$ MEFs (Figure 3A). Because this antibody recognizes all three Dvl isoforms (Dvl1–3) in mammals [4], we also performed immunoblotting analyses using specific antibodies against each Dvl isoform. As shown in Figure 3B, we could confirm that Dvl2 and Dvl3 are expressed in MEFs and that the protein levels of both of them are similarly reduced in *NRX*$^{-/-}$ MEFs. We then examined the ability of these MEFs to activate Wnt/β-catenin signaling in response to exogenously added Wnt ligands. The amount of active β-catenin increased in *NRX*$^{+/+}$ MEFs upon Wnt3a-conditioned medium (Wnt3a CM) treatment, but no significant changes were observed in the *NRX*$^{-/-}$ MEFs (Figure 3A). We also performed reporter assays and reverse transcriptase-polymerase chain reaction analyses to examine the downstream activation. As shown in Figures 3C and 3D, the reporter activity and target gene expression were increased in *NRX*$^{+/+}$ MEFs upon Wnt stimulation, but not in *NRX*$^{-/-}$ MEFs. When we introduced the NRX-expression vector to restore the expression of NRX

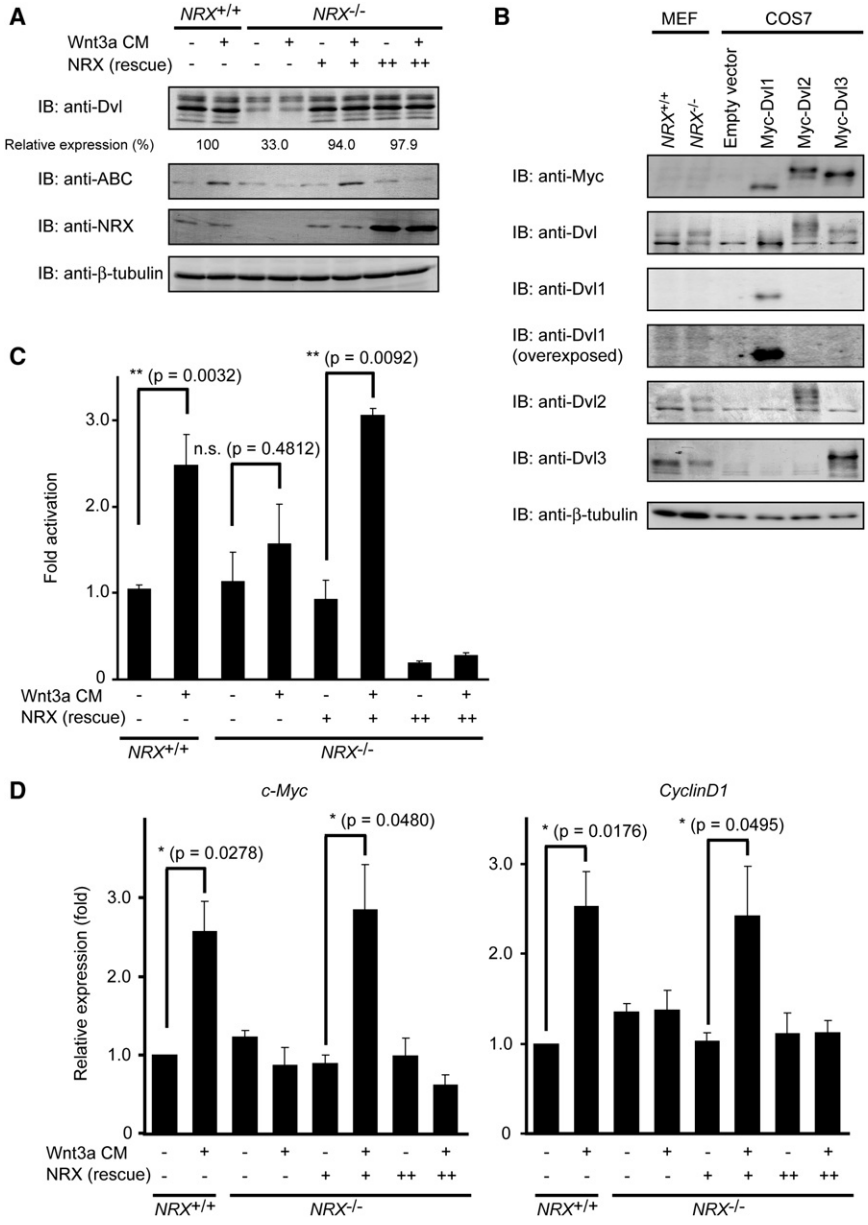

Figure 3. Impaired Activation of Wnt/β-Catenin Signaling in $NRX^{-/-}$ Mouse Embryonic Fibroblasts

(A) $NRX^{+/+}$ and $NRX^{-/-}$ mouse embryonic fibroblasts (MEFs) were transfected with nucleoredoxin (NRX) expression vector (0.1 μg [+] or 2 μg [++], filled with empty vector to total 2 μg). The cells were treated with Wnt3a-conditioned medium (Wnt3a CM, +) or control CM (−), and the lysates were subjected to immunoblotting with the indicated antibodies. Relative expression levels of the Dvl proteins are also indicated by normalizing the levels in $NRX^{+/+}$ samples to 100.

(B) Lysates of $NRX^{+/+}$ and $NRX^{-/-}$ MEFs, along with lysates of COS7 cells ectopically expressing Myc-Dvl1, Myc-Dvl2, or Myc-Dvl3, were subjected to immunoblotting with the indicated antibodies.

(C) MEFs were transfected with reporter vectors (TOPFLASH or FOPFLASH) and NRX expression vector, and the T cell factor (TCF)/lymphoid enhancer factor (LEF) activity of MEFs treated with Wnt3a CM (+) or control CM (−) was determined by luciferase assays (mean ± SE, n = 5), as reported previously [4]. p values were determined by the two-tailed Student's t test (paired). *p < 0.05.

(D) cDNAs prepared from MEFs treated as in (A) were subjected to real-time PCR analyses as a template to examine the expression levels of *c-Myc* and *CyclinD1*. The relative expression levels are shown as mean ± SE (n = 4). p values were determined by the two-tailed Student's t test (paired). *p < 0.05.

in the $NRX^{-/-}$ MEFs, the cells regained their potential to respond to Wnt stimulation (Figures 3A, 3C, and 3D), confirming that the impaired response of $NRX^{-/-}$ MEFs against Wnt stimulation was caused by loss of NRX. Notably, much stronger expression of NRX produced an opposite effect; the MEFs did not respond to Wnt at all (Figures 3A, 3C, and 3D). This is consistent with the original finding that overexpression of NRX blocks the Wnt-induced accumulation of β-catenin [4].

NRX Inhibits Dvl Ubiquitination by KLHL12

Previous studies indicated that NRX plays an inhibitory role in Wnt/β-catenin signaling, but our results obtained with $NRX^{-/-}$ MEFs clearly highlight an opposite role. This difference may be related to the stability of the Dvl proteins. Therefore, we performed pulse-chase analyses and identified a clear decrease in the half-life of the Dvl proteins in $NRX^{-/-}$ MEFs (from 14.8 hr to 7.6 hr, Figure 4A), indicating that Dvl degradation is accelerated in $NRX^{-/-}$ MEFs. Dvl directly interacts with Kelch-like 12 (KLHL12) in response to Wnt stimulation and is targeted for ubiquitination by the E3 complex, composed of Rbx1, Cullin3, and KLHL12 [3]. Therefore, we next examined the ubiquitination status of Dvl. When we treated MEFs with a proteasome inhibitor, MG132, the ubiquitination signal of Dvl was observable in $NRX^{+/+}$ MEFs. In contrast, the level of Dvl ubiquitination was found to be much higher in $NRX^{-/-}$ MEFs (Figure 4B). Wnt3a CM treatment significantly raised the ubiquitination level of Dvl in $NRX^{+/+}$ MEFs. However, we did not observe a similar increase with stimulation of Wnt3a in $NRX^{-/-}$ MEFs, probably because significant ubiquitination had already occurred, irrespective of Wnt3a stimulation. Next, we performed immunoprecipitation analyses to examine the status of complex formation between Dvl and KLHL12. The Dvl-KLHL12 interaction was found to be augmented by Wnt3a stimulation in $NRX^{+/+}$ MEFs. This is consistent with the previous report [3], but a high-level interaction was found to occur constitutively in $NRX^{-/-}$ MEFs, even though the levels of Dvl were lower (Figure 4C). To further confirm the importance of KLHL12 in the regulation of Dvl stability, we performed small interfering RNA (siRNA)-mediated knockdown analyses against KLHL12. As shown in Figure 4D, knockdown of KLHL12 resulted in a significant increase in the Dvl protein levels in MEF cells, especially in $NRX^{-/-}$ MEFs. Collectively, NRX appeared to function antagonistically with respect to KLHL12 to inhibit ubiquitination of Dvl.

NRX Expels KLHL12 from Dvl

The previous report indicated that KLHL12 directly associates with the C-terminal region of Dvl, but the central PDZ domain-containing region of Dvl is also important for a strong interaction [3]. NRX also directly binds to the central PDZ domain [4], and we thus speculated that NRX might compete with KLHL12 for Dvl and inhibit ubiquitination. To test this hypothesis, we purified recombinant proteins of GST-Dvl1-His, His-NRX, and His-KLHL12 and performed GST pull-down assays. We found that the addition of His-NRX could expel His-KLHL12 from the precipitate with GST-Dvl1-His (Figure 4E). The addition of His-NRX-mut, which lacks binding affinity for Dvl1 [4], showed no effect. We then performed in vitro ubiquitination assays to confirm that the direct ubiquitination of Dvl by the Rbx1/Cullin3/KLHL12 E3 complex is suppressed by NRX. For this purpose, Rbx1, Cullin3, and KLHL12 proteins were expressed in COS7 cells and purified by immunoprecipitation. Substrates such as ubiquitin and GST-Dvl1-His, together with other E1 and E2 proteins, were then added to initiate the ubiquitination reaction. We observed smear-positive signals of Dvl1 in the higher molecular weight region. The ubiquitin-conjugated form was confirmed by anti-Dvl immunoprecipitation and subsequent anti-ubiquitin immunoblotting. When we added His-NRX, most of the ubiquitinated form of Dvl1 disappeared, whereas addition of His-NRX-mut had no effect (Figure 4F). These results clearly indicate that NRX binds to Dvl1 and protects it from ubiquitination by inhibiting the interaction with KLHL12. We confirmed that both Dvl2 and Dvl3 can also associate with NRX as Dvl1 (Figure 4G). This result suggests the possibility that the stabilities of all Dvl isoforms are regulated by the interaction with NRX, which is consistent with the reduction of the protein levels of Dvl2 and Dvl3 in *NRX*$^{-/-}$ MEFs (Figure 3B). As shown in Figure 4C, Wnt3a stimulation strengthens the complex formation between Dvl and KLHL12, suggesting that the interaction of NRX with Dvl might be dynamically regulated. Indeed, coimmunoprecipitation analyses showed that the amount of the NRX-Dvl complex was decreased by Wnt3a stimulation (Figure 4H), which presumably contributes to the promotion of ubiquitination and degradation of Dvl by KLHL12.

The results shown in Figure 2C indicate that the amount of endogenous Dvl was significantly reduced in cardiac cells obtained from *NRX*$^{-/-}$ embryos, without a significant difference in osteoblasts. The immunoblotting analyses showed that the levels of KLHL12 were much higher in cardiac cells than in osteoblasts (Figure 2C), which might explain the difference in the levels of Dvl protein in the absence of NRX.

Conclusions

We previously reported that NRX inhibits Dvl function [4]. Consistent with this view, osteoblasts obtained from *NRX*$^{-/-}$ mice significantly activated Wnt/β-catenin signaling (Figure 1C). However, the signaling activity was paradoxically decreased in cardiocytes of *NRX*$^{-/-}$ mice (Figures 2C and 2D). These contradictory findings led to the discovery of the novel role of NRX as a Dvl stabilizer.

Dysregulation of Wnt/β-catenin signaling is a major cause of tumorigenesis. It should be noted that Dvl overexpression—often observed in cancer cells [1]—can aberrantly activate downstream signaling. In addition, it was recently reported that ATDC protein stimulates proliferation of pancreatic cancer cells by stabilizing and increasing Dvl levels [2]. Normal cells should thus be capable of regulating Dvl expression, and this regulation may occur via KLHL12-mediated ubiquitination system. On the other hand, sufficient Dvl levels are required to activate the signal pathway following Wnt stimulation. In such a delicately balanced situation, the competition between NRX and KLHL12 for Dvl provides appropriate regulation. In the resting state, NRX interacts with Dvl and blocks Dvl-KLHL12 interaction to maintain a pool of inactive Dvl, which is responsive to Wnt stimulation. Wnt stimulation then frees Dvl from its association with NRX and induces the activation of downstream signaling. Such NRX-free Dvl is vulnerable to ubiquitination by KLHL12 and subsequent degradation, thus avoiding persistent activation of Wnt/β-catenin signaling.

Experimental Procedures

Targeted Disruption of *NRX* Gene

We used phage clones obtained from mouse 129/SvJ strain-derived genomic library to generate the targeting vector. A linearized targeting vector was electroporated into E14.1 embryonic stem (ES) cells, and a portion of exon 3 and the entirety of exon 4 were replaced with a gene cassette containing *LacZ* and neomycin-resistant genes. Southern blot analyses were performed to confirm the proper recombination. The genomic DNAs were digested with *Hind*III and hybridized with the 5′ or 3′ probes. Correctly targeted ES clones were used to generate germline chimeras that were bred with C57BL/6J females.

Isolation of Osteoblast Precursor Cells and MEFs

Primary osteoblast precursors were isolated as previously reported [6], with the following minor modifications. Cells were isolated from calvaria of E18.5 *NRX*$^{+/+}$ or *NRX*$^{-/-}$ mice and were cultured in media (Dulbecco's modified Eagle's medium plus 10% fetal bovine serum) supplemented with 100 μg/ml ascorbic acid and 4 mM β-glycerophosphate. Differentiated osteoblasts were detected by the alkaline phosphatase method, as previously described [6]. Primary MEFs were isolated from E14.5 *NRX*$^{+/+}$ or *NRX*$^{-/-}$ mice and cultured by the standard method described elsewhere [20]. Plasmids and siRNAs were transfected into MEFs using the Neon transfection system (Invitrogen). Duplex siRNAs against mouse KLHL12 were from Invitrogen, which targets the following sequences: KLHL12-siRNA1, 5′- GGACUUCGUGUACACAGAAACAGUA-3′; KLHL12-siRNA2, 5′-CCGCCUCAGUUCGGUGGAAUGUCUA-3′; negative control, 5′-AAAUGGCGUCGCGUUCCUUUAGAGG-3′.

cDNAs

cDNAs of NRX, both wild type and mut (Cys205/208Ser), were generated in the previous study [4]. cDNAs of all Dvl isoforms (Dvl1, Dvl2, and Dvl3) were also generated in the previous study [4]. cDNAs of human KLHL12, Cullin3, and Rbx1 were obtained by PCR using a cDNA library of HEK293 cells as a template. The cDNA probe for Pitx2 was kindly provided by H. Shiratori and H. Hamada [21].

Antibodies

Anti-Dvl and anti-NRX rabbit polyclonal antibodies were generated in the previous study [4]. The following commercially available antibodies were also used: mouse monoclonal antibodies against active β-catenin (Millipore), β-tubulin (Sigma), smooth muscle actin (Sigma), Dvl1 (Santa Cruz), Dvl3 (Santa Cruz), ubiquitin (Santa Cruz), and FLAG-tag (Sigma); rabbit polyclonal antibodies against Runx2 (Santa Cruz), p75NTR (Promega), Dvl2 (Cell Signaling), and Myc-tag (Santa Cruz); goat polyclonal antibody against collagen I (Southern Biotechnology Associates); and chick polyclonal antibody against KLHL12 (Abcam).

Immunohistochemistry of Mouse Embryos

The immunohistochemistry of whole-mouse embryos was performed as previously described [22, 23], with the following minor modifications. Embryos were fixed with ice-cold 2% paraformaldehyde (PFA) in phosphate-buffered saline (PBS) for 10 min. They were then blocked twice in 2% skim milk, 0.2% bovine serum albumin, and 0.3% Triton X-100 in ice-cold PBS for 1 hr. For immunohistochemistry of sections, frozen sections of E18.5 mouse embryos were fixed in 4% PFA in PBS for 20 min. The immunostaining was performed as previously reported [24].

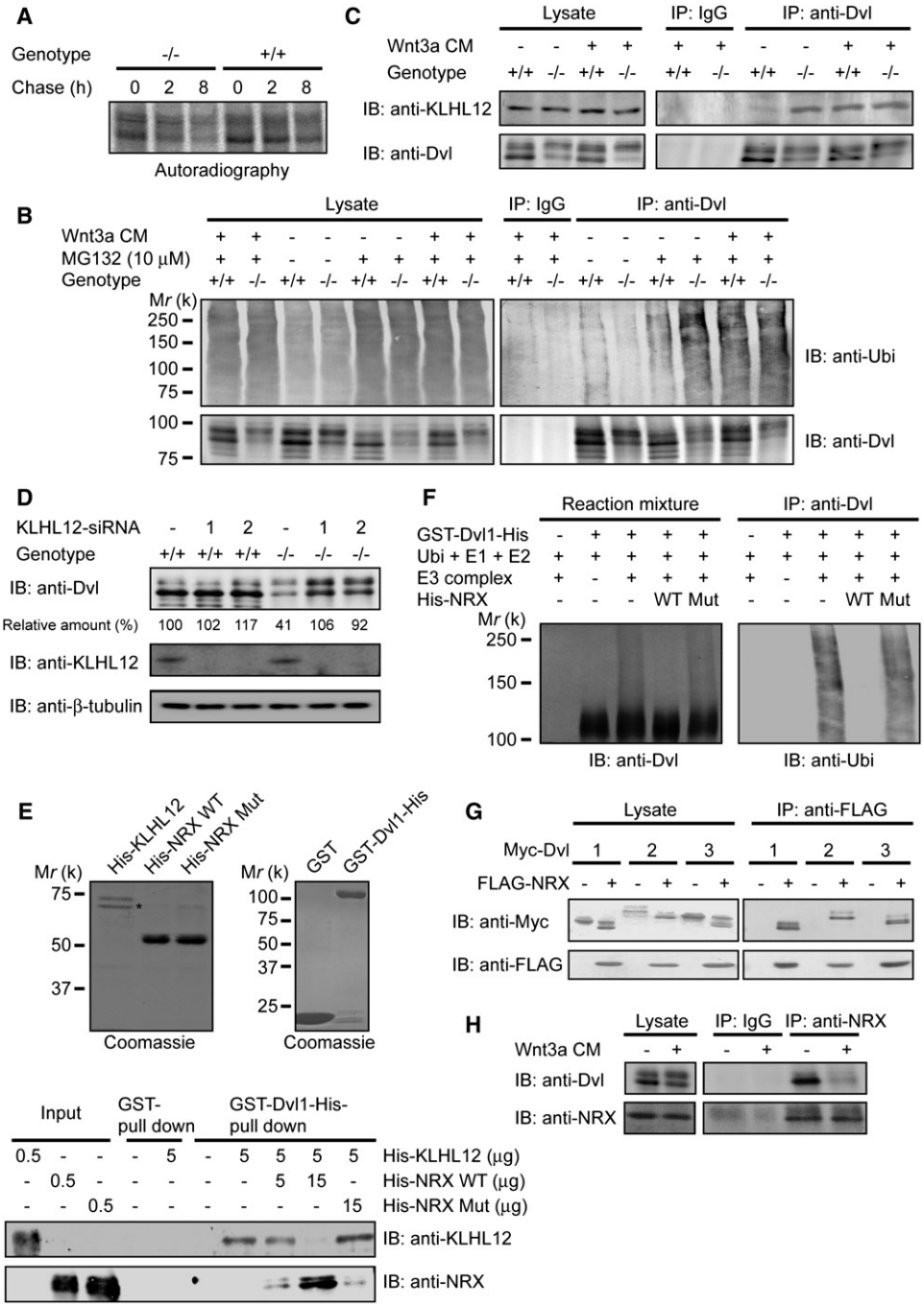

Figure 4. NRX Competes with KLHL12 to Suppress the Ubiquitination of Dvl

(A) Proteins in *NRX*$^{+/+}$ and *NRX*$^{-/-}$ MEFs were pulse-labeled with ^{35}S and then cultured for the indicated time periods. Dvl was immunoprecipitated and subjected to autoradiography.

(B) MEFs were treated with Wnt3a CM (+) or control CM (−) and with MG132 (or vehicle) for 10 hr, and the lysates were subjected to immunoprecipitation with anti-Dvl antibody, followed by immunoblotting with the indicated antibodies.

(C) MEFs were treated with Wnt3a CM (+) or control CM (−) for 10 hr, and their lysates were subjected to immunoprecipitation with anti-Dvl antibody. The precipitates were analyzed by immunoblotting with the indicated antibodies.

(D) MEFs were transfected with small interfering RNA (siRNA) against KLHL12 (1 or 2) or with control siRNA (−), and their lysates were subjected to immunoblotting with the indicated antibodies. Relative amounts of the Dvl proteins are also indicated by normalizing the levels of sample from control siRNA-transfected *NRX*$^{+/+}$ MEF to 100.

(E) Recombinant His-KLHL12 (expressed in bacteria), His-NRX (bacteria), and GST-Dvl1-His (insect cells) were purified, and the indicated amounts were subjected to GST pull-down assays. The purity of the recombinant proteins was assessed by Coomassie staining. * denotes nonspecifically purified protein that does not bind to Dvl.

(F) Recombinant GST-Dvl1-His proteins were subjected to in vitro ubiquitination assays with or without His-NRX (wild-type [WT] or Mut) proteins. The reaction mixtures were then subjected to direct immunoblotting with anti-Dvl antibody or immunoprecipitation with anti-Dvl antibody, followed by anti-Ubi immunoblotting.

In Vitro Ubiquitination Assays

In vitro ubiquitination assays of recombinant Dvl1 proteins were performed as previously described [3], with the following minor modifications. E3 complex components (FLAG-KLHL12, Myc-Cullin3, and Myc-Rbx1) were ectopically expressed in COS7 cells and purified by anti-FLAG immunoprecipitation. The complex was incubated for 2 hr at 37°C with 2 μg of purified GST-Dvl1-His proteins, 20 μg ubiquitin (Sigma), 100 ng E1 (His-UBE1, Boston Biochem), and 1 μg E2 (GST-UbcH5a, Boston Biochem).

Microarray Analyses

Microarray analyses were performed according to previous studies [25, 26]. Total RNAs were extracted from E9.5 and E11.5 embryos derived from $NRX^{+/+}$ and $NRX^{-/-}$ mice by using the RNeasy extraction kit (QIAGEN). Two dye-swapped experiments were performed by hybridizing complimentary RNA (cRNA) labeled with either Cy-3 or Cy-5 (Perkin-Elmer) onto a Whole Mouse Genome Oligo Microarray (G4122A; Agilent Technologies). The signature genes ($p < 0.05$, two-tailed Student's t test, paired) with mean fold changes > +2.0 (more than twice) or < −2.0 (less than half; + indicates upregulated and − indicates downregulated for each absolute value) at both stages were subjected to further evaluation.

Real-Time Polymerase Chain Reaction

Real-time polymerase chain reaction (PCR) experiments were performed with MiniOpticon (Bio-Rad) using the iQ SYBR green Supermix (Bio-Rad). The quality of the final PCR product was checked by agarose gel electrophoresis, and it was confirmed that there were no obvious nonspecifically amplified DNAs. The primers used are as follows: *Fzd2* (5′-CGCTTCCG TTCCCTTCTCTC-3′ and 5′-ACACATAACACACAACCCAATCC-3′), *Fgf10* (5′-CAGTAAGACACGCAAGCATTTACTG-3′ and 5′-AATCTGATCCAATTCTT CCATGGT-3′), *Isl1* (5′-TAAGCATGCCTGTAGCTGGTT-3′ and 5′-GATGGAT CTCAAAAAAATGGTAAAGAG-3′), *Hand2* (5′-CCACCAGATACATCGCCTAC CT-3′ and 5′-CTTTCACGTCGGTCTTCTTGATC-3′), *Tgfb2* (5′-GCGAAGAG CTCGAGGCGAGAT-3′ and 5′-GAGAATGGTCAGTGGTTCCAGAT-3′), and *HSPG2* (5′- TGATGCCCCTGGGCAATACGG-3′ and 5′-CTGTGCTGGTCC GAACCTCG-3′). The primers for *c-Myc*, *Cyclin D1*, and *GAPDH* were described previously [4].

Accession Numbers

The microarray data have been deposited in the Gene Expression Omnibus (NCBI-GEO) database under accession number GSE21954.

Supplemental Information

Supplemental Information includes two figures and can be found with this article online at doi:10.1016/j.cub.2010.09.065.

Acknowledgments

We thank H. Shiratori and H. Hamada (Osaka University) for the WISH probe for *Pitx2* and technical advice for WISH experiments, as well as D. Yamazaki (Kobe University), K. Sekiguchi, and K. Yoshikawa (Osaka University) for technical advice for immunohistochemistry experiments. This study was supported in part by a Grant-in-Aid for Scientific Research from the Japan Society for the Promotion of Science and from the Ministry of Education, Culture, Sports, Science and Technology, Japan.

Received: July 19, 2010
Revised: September 10, 2010
Accepted: September 29, 2010
Published online: October 21, 2010

References

1. Uematsu, K., Kanazawa, S., You, L., He, B., Xu, Z., Li, K., Peterlin, B.M., McCormick, F., and Jablons, D.M. (2003). Wnt pathway activation in mesothelioma: Evidence of Dishevelled overexpression and transcriptional activity of beta-catenin. Cancer Res. *63*, 4547–4551.
2. Wang, L., Heidt, D.G., Lee, C.J., Yang, H., Logsdon, C.D., Zhang, L., Fearon, E.R., Ljungman, M., and Simeone, D.M. (2009). Oncogenic function of ATDC in pancreatic cancer through Wnt pathway activation and beta-catenin stabilization. Cancer Cell *15*, 207–219.
3. Angers, S., Thorpe, C.J., Biechele, T.L., Goldenberg, S.J., Zheng, N., MacCoss, M.J., and Moon, R.T. (2006). The KLHL12-Cullin-3 ubiquitin ligase negatively regulates the Wnt-beta-catenin pathway by targeting Dishevelled for degradation. Nat. Cell Biol. *8*, 348–357.
4. Funato, Y., Michiue, T., Asashima, M., and Miki, H. (2006). The thioredoxin-related redox-regulating protein nucleoredoxin inhibits Wnt-beta-catenin signalling through dishevelled. Nat. Cell Biol. *8*, 501–508.
5. Boles, M.K., Wilkinson, B.M., Wilming, L.G., Liu, B., Probst, F.J., Harrow, J., Grafham, D., Hentges, K.E., Woodward, L.P., Maxwell, A., et al. (2009). Discovery of candidate disease genes in ENU-induced mouse mutants by large-scale sequencing, including a splice-site mutation in nucleoredoxin. PLoS Genet. *5*, e1000759.
6. Yu, H.M., Jerchow, B., Sheu, T.J., Liu, B., Costantini, F., Puzas, J.E., Birchmeier, W., and Hsu, W. (2005). The role of Axin2 in calvarial morphogenesis and craniosynostosis. Development *132*, 1995–2005.
7. Liu, K.J., Arron, J.R., Stankunas, K., Crabtree, G.R., and Longaker, M.T. (2007). Chemical rescue of cleft palate and midline defects in conditional GSK-3beta mice. Nature *446*, 79–82.
8. Cheng, J.H., She, H., Han, Y.P., Wang, J., Xiong, S., Asahina, K., and Tsukamoto, H. (2008). Wnt antagonism inhibits hepatic stellate cell activation and liver fibrosis. Am. J. Physiol. Gastrointest. Liver Physiol. *294*, G39–G49.
9. Tice, D.A., Szeto, W., Soloviev, I., Rubinfeld, B., Fong, S.E., Dugger, D.L., Winer, J., Williams, P.M., Wieand, D., Smith, V., et al. (2002). Synergistic induction of tumor antigens by Wnt-1 signaling and retinoic acid revealed by gene expression profiling. J. Biol. Chem. *277*, 14329–14335.
10. Morkel, M., Huelsken, J., Wakamiya, M., Ding, J., van de Wetering, M., Clevers, H., Taketo, M.M., Behringer, R.R., Shen, M.M., and Birchmeier, W. (2003). Beta-catenin regulates Cripto- and Wnt3-dependent gene expression programs in mouse axis and mesoderm formation. Development *130*, 6283–6294.
11. van Gijn, M.E., Blankesteijn, W.M., Smits, J.F., Hierck, B., and Gittenberger-de Groot, A.C. (2001). Frizzled 2 is transiently expressed in neural crest-containing areas during development of the heart and great arteries in the mouse. Anat. Embryol. (Berl.) *203*, 185–192.
12. Hamblet, N.S., Lijam, N., Ruiz-Lozano, P., Wang, J., Yang, Y., Luo, Z., Mei, L., Chien, K.R., Sussman, D.J., and Wynshaw-Boris, A. (2002). Dishevelled 2 is essential for cardiac outflow tract development, somite segmentation and neural tube closure. Development *129*, 5827–5838.
13. Etheridge, S.L., Ray, S., Li, S., Hamblet, N.S., Lijam, N., Tsang, M., Greer, J., Kardos, N., Wang, J., Sussman, D.J., et al. (2008). Murine dishevelled 3 functions in redundant pathways with dishevelled 1 and 2 in normal cardiac outflow tract, cochlea, and neural tube development. PLoS Genet. *4*, e1000259.
14. Raible, D.W., and Ragland, J.W. (2005). Reiterated Wnt and BMP signals in neural crest development. Semin. Cell Dev. Biol. *16*, 673–682.
15. Snider, P., Olaopa, M., Firulli, A.B., and Conway, S.J. (2007). Cardiovascular development and the colonizing cardiac neural crest lineage. ScientificWorldJournal *7*, 1090–1113.
16. Eisenberg, L.M., and Eisenberg, C.A. (2006). Wnt signal transduction and the formation of the myocardium. Dev. Biol. *293*, 305–315.
17. Cohen, E.D., Wang, Z., Lepore, J.J., Lu, M.M., Taketo, M.M., Epstein, D.J., and Morrisey, E.E. (2007). Wnt/beta-catenin signaling promotes expansion of Isl-1-positive cardiac progenitor cells through regulation of FGF signaling. J. Clin. Invest. *117*, 1794–1804.
18. Zhou, W., Lin, L., Majumdar, A., Li, X., Zhang, X., Liu, W., Etheridge, L., Shi, Y., Martin, J., Van de Ven, W., et al. (2007). Modulation of morphogenesis by noncanonical Wnt signaling requires ATF/CREB family-mediated transcriptional activation of TGFbeta2. Nat. Genet. *39*, 1225–1234.
19. Habas, R., Dawid, I.B., and He, X. (2003). Coactivation of Rac and Rho by Wnt/Frizzled signaling is required for vertebrate gastrulation. Genes Dev. *17*, 295–309.

(G) COS7 cells were transfected with the indicated expression constructs, and their lysates were subjected to immunoprecipitation with anti-FLAG antibody. The precipitates were analyzed by immunoblotting with the indicated antibodies.
(H) MEFs were treated with Wnt3a CM (+) or control CM (−) for 10 hr, and their lysates were subjected to immunoprecipitation with anti-NRX antibody. The precipitates were analyzed by immunoblotting with the indicated antibodies.

20. Parrinello, S., Samper, E., Krtolica, A., Goldstein, J., Melov, S., and Campisi, J. (2003). Oxygen sensitivity severely limits the replicative lifespan of murine fibroblasts. Nat. Cell Biol. *5*, 741–747.
21. Yoshioka, H., Meno, C., Koshiba, K., Sugihara, M., Itoh, H., Ishimaru, Y., Inoue, T., Ohuchi, H., Semina, E.V., Murray, J.C., et al. (1998). Pitx2, a bicoid-type homeobox gene, is involved in a lefty-signaling pathway in determination of left-right asymmetry. Cell *94*, 299–305.
22. Yamazaki, D., Suetsugu, S., Miki, H., Kataoka, Y., Nishikawa, S., Fujiwara, T., Yoshida, N., and Takenawa, T. (2003). WAVE2 is required for directed cell migration and cardiovascular development. Nature *424*, 452–456.
23. Kuwako, K., Hosokawa, A., Nishimura, I., Uetsuki, T., Yamada, M., Nada, S., Okada, M., and Yoshikawa, K. (2005). Disruption of the paternal necdin gene diminishes TrkA signaling for sensory neuron survival. J. Neurosci. *25*, 7090–7099.
24. Satoh, W., Gotoh, T., Tsunematsu, Y., Aizawa, S., and Shimono, A. (2006). Sfrp1 and Sfrp2 regulate anteroposterior axis elongation and somite segmentation during mouse embryogenesis. Development *133*, 989–999.
25. Ishii, T., Onda, H., Tanigawa, A., Ohshima, S., Fujiwara, H., Mima, T., Katada, Y., Deguchi, H., Suemura, M., Miyake, T., et al. (2005). Isolation and expression profiling of genes upregulated in the peripheral blood cells of systemic lupus erythematosus patients. DNA Res. *12*, 429–439.
26. Oneyama, C., Hikita, T., Nada, S., and Okada, M. (2008). Functional dissection of transformation by c-Src and v-Src. Genes Cells *13*, 1–12.